Polymer 52 (2011) 3704–3709

Contents lists available at ScienceDirect

Polymer

journal homepage: www.elsevier.com/locate/polymer

Synthesis and characterization of all-conjugated diblock copolymers consisting of thiophenes with a hydrophobic alkyl and a hydrophilic alkoxy side chain

Jinseck Kim [1], Ayyanar Siva [2], In Young Song, Taiho Park*

Department of Chemical Engineering, Polymer Research Institute, Pohang University of Science and Technology, Pohang 790-784, Republic of Korea

A R T I C L E I N F O

Article history:
Received 26 March 2011
Received in revised form
14 June 2011
Accepted 19 June 2011
Available online 25 June 2011

Keywords:
Conjugated diblock copolymer
Thiophene
Grignard metathesis polymerization

A B S T R A C T

Novel thiophene-based all-conjugated block copolymers consisting of 3-hexylthiophene and 3-{2-[2-(2-methoxyethoxy)ethoxy]ethoxy}thiophene were synthesized using the Grignard metathesis (GRIM) polymerization method in the presence of Ni(dppp)Cl_2. Favorable transfer of the catalytic site from an electron-poor precursor to an electron-rich monomer was found to produce the block copolymer. The molecular weights of the copolymers increased slightly with increasing polymerization temperature (10.1×10^3 M_n (35 °C) → 11.1×10^3 M_n (55 °C)), suggesting that transit of the catalytic site was accelerated at high temperatures. Size exclusion chromatography, UV–vis and photoluminescence spectroscopies, and cyclic voltammetry measurements confirmed that the polymers were block copolymers. The blocks were associated and organized relative to one another in adjacent chains.

1. Introduction

Since McCullough developed the Grignard metathesis (GRIM) polymerization [1] of poly(3-hexylthiophenes) (P3HT), P3HT has been employed widely in organic electronic and photonic applications, such as organic field-effect transistors (OFETs) [2] and organic photovoltaic (OPV) devices [3]. These materials display relatively high hole mobilities ($\mu_h = 10^{-2}$ cm^2 V^{-1} s^{-1}) and low bandgaps ($\Delta E_g = 1.9$ eV) [4]. A product of the GRIM polymerization method was prepared by magnesium halogen exchange of 2,5-dibromo-3-hexylthiophene with CH_3MgCl followed by addition of a Ni catalyst to afford P3HTs with a narrow molecular weight distribution and high regioregularity. Extensive independent studies of the polymerization mechanism by McCullough [5] and Yokozawa [6] revealed that the polymerization reaction displayed characteristics reminiscent of a quasi-living process. Tajima et al. [7] and others [8] have described the successful synthesis of thiophene-based all-conjugated diblock copolymers, such as poly(3HT-*b*-(3(2-ethylhexyl)thiophene)) [7] (**1**) as a crystalline-amorphous diblock copolymer, and poly(3HT-*b*-(3(4-octylphenyl)thiophene)) [8a] (**2**) and poly(-(3-buylthiophene)-*b*-(3-octylthiophene)) [8b] (**3**) as crystalline–crystalline diblock copolymers. This novel method was extended to monomers other than thiophene and its derivatives, such as 1,4-dibromo-2,5-dialkoxy-benzene (**5**) [9], 2,5-dibromo-1-alkyl-1*H*-pyrrole [10], 2,7-dibromo-N-alkyl-substituted carbazole [11], and 2,7-dibromo-9-dialkylfluorene [11]. During the propagation step, reductive elimination yielded a thiophene–thiophene bond via intramolecular transfer of the nickel to the chain end by oxidative insertion into the thiophene-bromine bond. Therefore, controlling intramolecular transfer was a key to obtain a well-defined block copolymer with a narrow molecular weight distribution. Yokozawa et al. demonstrated that the order of addition of the monomers played a crucial role in the successful transfer of the catalyst from one block to the next [9]. The initial polymerization of the more strongly π-rich thiophene monomer, followed by addition of the *p*-phenylene monomer, resulted in a broad molecular weight distribution. Meanwhile, reversing the order of polymerization led to well-controlled polymerization with a narrow molecular weight distribution. Recently, we reported synthesis of a novel thiophene-based all-conjugated diblock copolymer (**4**) with hydrophobic and hydrophilic side chains. This polymer formed a polymeric vesicle with a crystalline interior and an amorphous exterior [12]. Herein, we report the synthesis of novel all-conjugated thiophene-based amphiphilic diblock copolymers. We used a second monomer [13] (**10**) with a {2-[2-(2-methoxyethoxy)ethoxy]ethoxy} side chain rather than an alkyl chain to produce a rod-rod-type amphiphilic diblock copolymer. This allowed us to investigate the intramolecular transfer of the catalyst from the growing chain end to the strongly π-rich thiophene monomer, in contrast with the case of **5**, as the

---

* Corresponding author. Tel.: +82 54 279 2394; fax: +82 54 279 8298.
E-mail addresses: drasiva@gmail.com (A. Siva), taihopark@postech.ac.kr (T. Park).

[1] Present address: LG Chem. Research Park, 104-1, Moonji-Dong, Yoseong-Gu, Daejeon 305-360, Republic of Korea.

[2] Present address: Department of Inorganic Chemistry, School of Chemistry, Madurai Kamaraj University, Palkalai Nagar, Madurai 625 021, Tamilnadu, India.

0032-3861/$ – see front matter © 2011 Elsevier Ltd. All rights reserved.
doi:10.1016/j.polymer.2011.06.030

alkoxy side chain enhanced the π-electron character of the thiophene. In addition, the copolymers were expected to show a broad white light absorption spectrum and a low bandgap due to the electron-rich side chain (Fig. 1).

2. Experimental details and measurements

2.1. Materials and reagents

2,5-Dibromo-3-hexylthiophene (**11**) and 2,5-dibromo-3-{2-[2-(2-methoxyethoxy)ethoxy]ethoxy}thiophene (**10**) were synthesized according to the previously reported procedures.[5d,13b] All other chemical reagents were purchased from Aldrich Co. and used without further purification except for tetrahydrofuran (THF) which is purified using a J.C. Meyer solvent dispensing system.

2.2. Characterization

^{1}H NMR spectra were recorded on a Bruker DPX-300 (300 MHz) FT NMR system operating at 300 MHz. Number-average (M_n) and weight-average (M_w) molecular weights were determined by size exclusion chromatography (SEC) using the SHIMADZU LC solution, chloroform as the eluent, and a calibration curve of polystyrene standards. The UV–Vis absorption spectra were measured using a Carry 5000 UV–Vis-near infrared double beam spectrophotometer, and photoluminescence (PL) spectra of the copolymers were measured on a Jasco FP-6500 spectrometer. Cyclic voltammetry was performed using a POWERLAB/AD instrument model system in a three-electrode cell with a 0.1 M Bu_4NBF_4 solution in acetonitrile at a scan rate of 50 mV s^{-1}. A glassy carbon disk (~0.05 cm^2) coated with a thin polymer film was used as the working electrode. A platinum wire and an $Ag/AgNO_3$ electrode were used as the counter- and reference electrodes, respectively. All measurements were calibrated against an internal standard of ferrocene (Fc), the ionization potential (IP) value of which is 4.8 eV for the Fc/Fc^+ redox system.

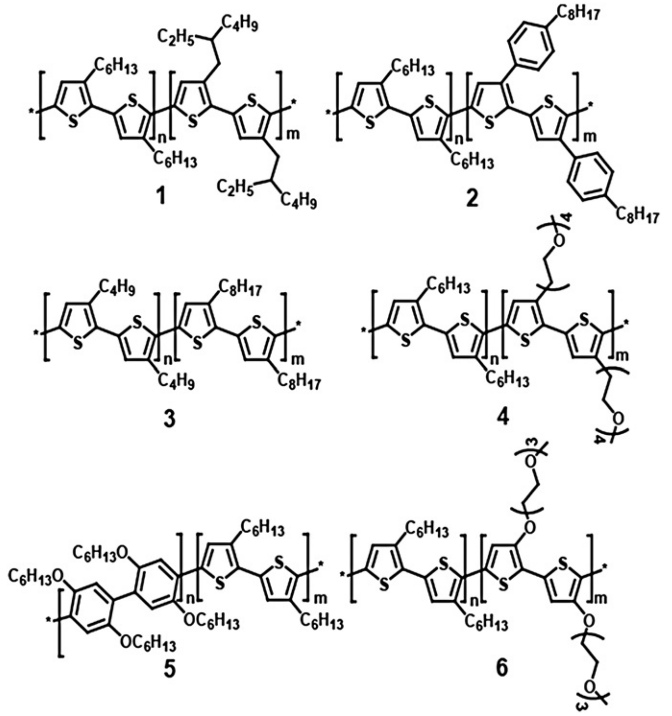

Fig. 1. Structures of the thiophene-based all-conjugated diblock copolymers reported in the literature (**1**–**5**) and synthesized here (**6**).

2.3. Poly(3-hexylthiophene), P3HT

Methylmagnesium bromide (5.3 mL, 1M solution in butylether, 5.25 mmol) was slowly added to a solution of 2,5-dibromo-3-hexylthiophene (1.63 g, 5 mmol) (**11**) in anhydrous THF (20 mL) at room temperature and the mixture was heated at 60 °C for 1 h. $Ni(dppp)Cl_2$ (14 mg, 0.025 mmol) dispersed in anhydrous THF(1 mL) was added and the solution was stirred at 60 °C for overnight. The mixture was poured into 200 mL of methanol and precipitate was filtered. Soxhlet extractions were performed with methanol (to remove monomer and salts), hexanes (to remove catalyst and oligomers), and chloroform. The chloroform fraction was reduced and dried in vacuo to afford 0.454 g (54%) of the title polymer as a violet film. ^{1}H NMR ($CDCl_3$): δ[ppm] 6.98 (s, 1H), 2.80 (t, 2H), 1.71 (m, 2H), 1.36 (m, 6H), 0.91 (t, 3H).

2.4. P3HT-b-PMET block copolymers **6**

Methylmagnesium bromide (4 mL, 1 M solution in bytylether, 4 mmol) was slowly added to a solution of 2,5-dibromo-3-hexylthiophene (1.30 g, 4 mmol) (**11**) in anhydrous THF (40 mL) at room temperature and the mixture stirred for 1 h. To the mixture was added a suspension of $Ni(dppp)Cl_2$ (43 mg, 0.08 mmol) in THF (1 mL) via a syringe, and the mixture was stirred at room temperature for 1 h. After this, solution mixture (1 mmol) (**13**) was transferred to the THF solutions of **14** which had been prepared by treatment of **10** (0.404 g, 1.00 mmol) in THF (10 mL) with methylmagnesium bromide (1 mL, 1 M solution in butylether, 1 mmol) at different temperatures (**BC1**: 35°, **BC2**: 45°, **BC3**: 55 °C). Each solution was stirred for overnight. The resulting mixtures were poured into 200 mL of methanol and precipitate was filtered. Soxhlet extractions were performed with methanol (to remove monomer and salts), hexanes (to remove catalyst and oligomers), and chloroform. The chloroform fraction was reduced and dried in vacuo and reprecipitated in methanol.

BC1: viscous violet colored solid, 125.3 mg (30% yield) ^{1}H NMR ($CDCl_3$): δ[ppm] 6.98 (br, 2.24H), 4.34 (br, 2.38H), 3.95 (br, 2.26H), 3.80–3.52 (m, 9.53H), 3.35 (br, 3.40H), 2.80 (br, 1.61H), 1.70 (br, 2.14H), 1.35 (br, 7.21H), 0.91 (br, 3.00H).

BC2: viscous violet colored solid, 172.3 mg (42% yield) ^{1}H NMR ($CDCl_3$): δ[ppm] 6.98 (br, 2.03H), 4.34 (br, 2.37H), 3.95 (br, 2.25H), 3.80–3.52 (m, 10.88H), 3.35 (br, 3.73H), 2.80 (br, 1.50H), 1.70 (br, 1.60H), 1.35 (br, 7.03H), 0.91 (br, 3.00H).

BC3: viscous violet colored solid, 171.6 mg (41% yield) ^{1}H NMR ($CDCl_3$): δ[ppm] 6.98 (br, 1.95H), 4.34 (br, 2.35H), 3.95 (br, 2.19H), 3.80–3.52 (m, 11.28H), 3.35 (br, 3.87H), 2.80 (br, 1.46H), 1.70 (br, 1.47H), 1.35 (br, 6.55H), 0.91 (br, 3.00H).

2.5. Poly(3-[2-[2(2-methoxyethoxy)ethoxy]ethoxy]thiophene) (PMET)

Methylmagnesium bromide (5.3 mL, 1 M solution in butylether, 5.25 mmol) was slowly added to a solution of 2,5-dibromo-3-{2-[2-(2-methoxyethoxy)ethoxy]ethoxy}thiophene (**10**) (2.00 g, 5 mmol) in anhydrous THF (20 mL) at room temperature and the mixture was heated at 60 °C for 1 h. $Ni(dppp)Cl_2$ (14 mg, 0.025 mmol) dispersed in anhydrous THF(1 mL) was added and the solution was stirred at 60 °C for overnight. The mixture was poured into 200 mL of methanol and precipitate was filtered. Soxhlet extractions were performed with methanol (to remove monomer and salts), hexanes (to remove catalyst and oligomers), and chloroform. The chloroform fraction was reduced and dried in vacuo to afford 0.467 g

(38%) of the title polymer as a violet colored solid. ^{1}H NMR ($CDCl_3$): δ[ppm] 6.98 (s, 1H), 4.34 (br, 2H), 3.95 (br, 2H), 3.80–3.52 (m, 10H), 3.35 (br, 3H).

3. Results and discussion

3.1. Synthesis and characterization

The synthesis of the monomers and block copolymers are outlined in Fig. 2. The thiophene-based derivative (**9**) having a hydrophilic 2-[2-(2-methoxyethoxy)ethoxy]ethoxy substituent was synthesized by copper (I)-mediated substitution of 3-bromothiophene (**7**), followed by NBS bromination in THF at cryogenic temperatures.

To prepare the amphiphilic block copolymers, the active hydrophobic GRIM product (**12**) was prepared *in situ* by magnesium halogen exchange of **11** (4.0 mmol) with CH_3MgBr, followed by polymerization at room temperature in the presence of a Ni catalyst (Ni(dppp)Cl_2) to obtain the P3HT living prepolymer (**13**) in the first step. Three separate solutions containing the hydrophilic active GRIM product (**14**) from **10** (1.0 mmol) were prepared by reaction with CH_3MgBr. Equal amounts (1.0 mmol) of the P3HT living prepolymer (**13**) were added to the three reaction solutions of the GRIM product (**14**) (1.0 mmol). Polymerization of the three identical compositions was conducted at 35, 45, and 55 °C overnight to afford the three block copolymers, **BC1**, **BC2**, and **BC3**, respectively. The polymerization results are summarized in Table 1. The polymer molecular weights and distributions (M_n/M_w) were determined by size exclusion chromatography (SEC) against polystyrene standards using $CHCl_3$ as the eluent.

Table 1
Molecular weights of the prepolymers, copolymers, and ratios of the blocks.

Polymers	Temp (°C)	10^3 M_n (g/mol) (M_n/M_w)[a]	Ratio (3HT:MET)[b]	
			by GPC[c]	by NMR[d]
P3HT Precursor (**13**)	r.t.	5.5 (1.24)	–	–
BC1	35	10.1 (1.64)	64:36	47:53
BC2	45	10.8 (1.68)	60:40	45:55
BC3	55	11.1 (1.73)	59:41	44:56
PMET	r.t.	21.4 (1.32)	–	–
P3HT	r.t.	38.6 (1.26)	–	–

[a] Determined by SEC in chloroform using a polystyrene standard.

[b] Indicates the molar ratio of the monomer units of the **11** (3HT) and **10** (MET) block polymers.

[c] Estimated from the molecular weights of the repeated units and the degree of polymerization in each block.

[d] Estimated from the integral of the proton peaks at 3.35 ($-OCH_3$) and 0.91 ($-CH_3$) ppm.

Fig. 3 shows the SEC chromatograms of the P3HT living prepolymer (**13**) and the resulting block copolymers. The molecular weight of the P3HT living prepolymer (**13**) was 5.5 *k*Da (M_n), which increased after reaction of the GRIM product (**14**) with the second monomer. The monomer apparently did not decompose, and the block copolymers were successfully synthesized. This result was observed despite the report of Murso et al. [14] that monomer decomposition occurred at high temperatures by reaction with CH_3Br generated in the metathesis reaction. Monomer decomposition also demonstrated that transferring of the catalytic site from a weaker electron-poor precursor (**13**) to a stronger electron-rich monomer (**14**) favored production of copolymers with narrow molecular weight distributions [9].

Interestingly, the molecular weights of the copolymers increased slightly with increasing polymerization temperature at the second step (10.1 × 10^3 M_n (35 °C) → 10.8 × 10^3 M_n (45 °C) → 11.1 × 10^3 M_n (55 °C)). This result suggested that transferring the catalytic site from the electron-poor precursor (**13**) to the electron-rich monomer, relatively, was accelerated at high temperatures. The temperature-dependent polymerization was consistent with reports in the literature [15]. The molecular weight distributions of the copolymers fell in the range 1.64–1.73 M_n/M_w, which was slightly larger than the distributions of the homopolymers, e.g., the P3HT prepolymer (1.24 M_n/M_w), P3HT (1.26 M_n/M_w) with a large molecular weight (38.6 × 10^3 M_n), or PMET (1.32 M_n/M_w). This was mainly ascribed to a shift toward a high molecular weight polymer distribution, as seen in Fig. 3.

The block ratios of the copolymers, calculated using the value for M_n obtained from SEC measurements, were in the range 64:36–59:41 (3HT:MET). This range was close to the expected value (50:50). On the other hand, the ratio estimated from ^{1}H-NMR

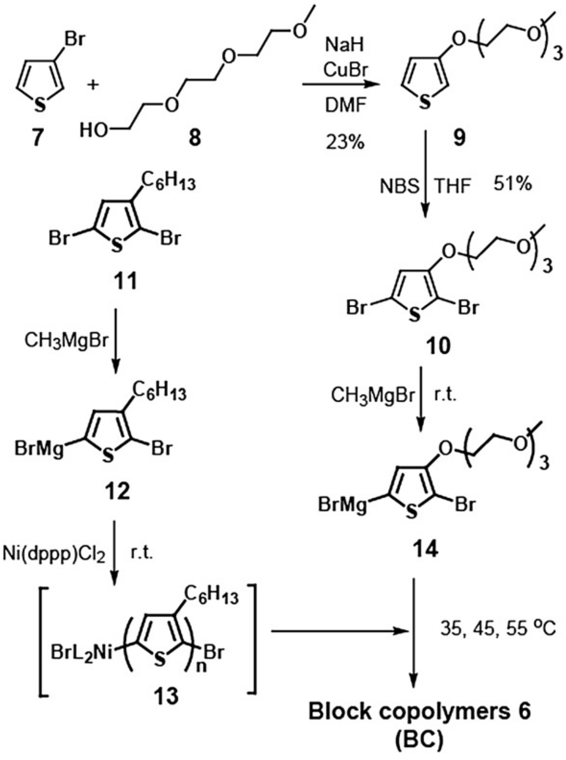

Fig. 2. Synthetic scheme for preparing the hydrophilic monomer (**10**), and the quasi-living copolymerization of the block copolymers (BC, 6) at various temperatures (35, 45, and 55 °C).

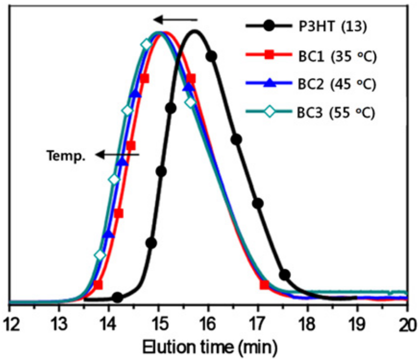

Fig. 3. GPC elution curves of the prepolymer (P3HT) **13** and the block copolymers **BC1**, **BC2**, and **BC3**.

spectra, in which a methoxy peak ($-OCH_3$) in the PMET block and a methyl peak ($-CH_3$) in the P3HT block appeared at 3.35 and 0.91 ppm, respectively, provided a range of 47:53–44:56 (3HT:MET). The value of M_n for the copolymers obtained from SEC measurements was relative and assumed a random coil configuration, and the ratios obtained from the ^{1}H NMR spectra may have been more reliable than those derived from SEC measurements. The expected values may have been sensitive to differences in the reactivities of the two monomers. Indeed, M_n (38.6 kDa M_n) for P3HT was larger than that (21.4 kDa M_n) of PMET under identical polymerization conditions.

3.2. Photophysical properties

To further investigate the structures and organizational association among blocks in adjacent chains, optical studies of the block copolymers were conducted in solution [1×10^{-5} M] and film using by UV–vis spectroscopy, as shown in Fig. 4 (Table 2). We couldn't observe any new peaks or changes of shapes up to this concentration [16]. The absorption maximum (A_{max}) of PMET was 578 nm in a chloroform solution (Fig. 4(a)) and 650 nm in the film state (Fig. 4(b)), higher than the values (450 nm in chloroform and 521 nm in film) for P3HT. This observation indicated that introducing an alkoxy side chain led to a lower bandgap due to the mesomeric effect [17]. Meanwhile, both homopolymers (P3HT and PMET) exhibited 71–72 nm red shifts at A_{max} in transitioning from solution to film, indicating that the increased effective conjugation length was governed not by the side chains, but by the nature of the main backbones of the homopolymers.

The full width at half-maximum of the absorption band of the block copolymer **BC1** (228 nm) was greater than the corresponding values for the homopolymers (P3HT = 123 nm and PMET = 145 nm) in chloroform (Fig. 4(a)). This was consistent with a structure in which the block copolymer contained intact P3HT and PMET units. The solid-state properties of the block copolymer were studied. Films were prepared by spin-casting, followed by annealing at three different temperatures (50, 100, and 150 °C), and the absorbance properties were measured. For PMET, A_{max} appeared at 650 nm at 35 °C, but it decreased slightly to 619 nm (Fig. 4(c)). For P3HT, the absorption spectra revealed an additional absorption peak at 610 nm. This peak originated from the P3HT crystalline structure, which featured π-π interactions among the P3HT blocks [18]. As the annealing temperature increased, an additional peak (610 nm) was observed (Fig. S1). Similar results were observed in the absorption spectra of **BC1** (Fig. 4(d)), (see Fig. S2 for **BC2** and **BC3**). The peak intensity at 610 nm was enhanced at higher annealing temperatures, indicating the preparation of two distinctive well-separated blocks, which associated with one another and organized the adjacent chains at high temperatures.

Table 2
UV–Vis absorption and emission data for P3HT, **BC1**, **BC3**, and PMET in chloroform and in film.

Polymers	Absorption				Emission	
	Solution ($CHCl_3$)		Film		Solution ($CHCl_3$)	Film
	A_{max}[a] (nm)	ΔE_{opt}[b] (eV)	A_{max}[a] (nm)	ΔE_{opt}[b] (eV)	λ_{max}[c] (nm)	λ_{max}[c] (nm)
P3HT	450	1.90	521	1.86	578	653
BC1	487	1.81	563	1.44	580	651
BC3	–	–	–	–	620	654
PMET	578	1.71	650	1.44	657	721

[a] Absorption maximum wavelength.
[b] Optical bandgap calculated at long wavelength absorption onset point.
[c] Photoluminescence (PL) maximum wavelength. Excited at 420 nm.

A comparison of the photoluminescence (PL) of P3HT, PMET, and the block copolymers clearly supported the association and organization among blocks in adjacent chains (Fig. 5). The emission maxima (λ_{max}) of PMET, excited at 420 nm, were 657 nm in chloroform (Fig. 5(a)) or 721 nm in film (Fig. 5(b)) and were higher than

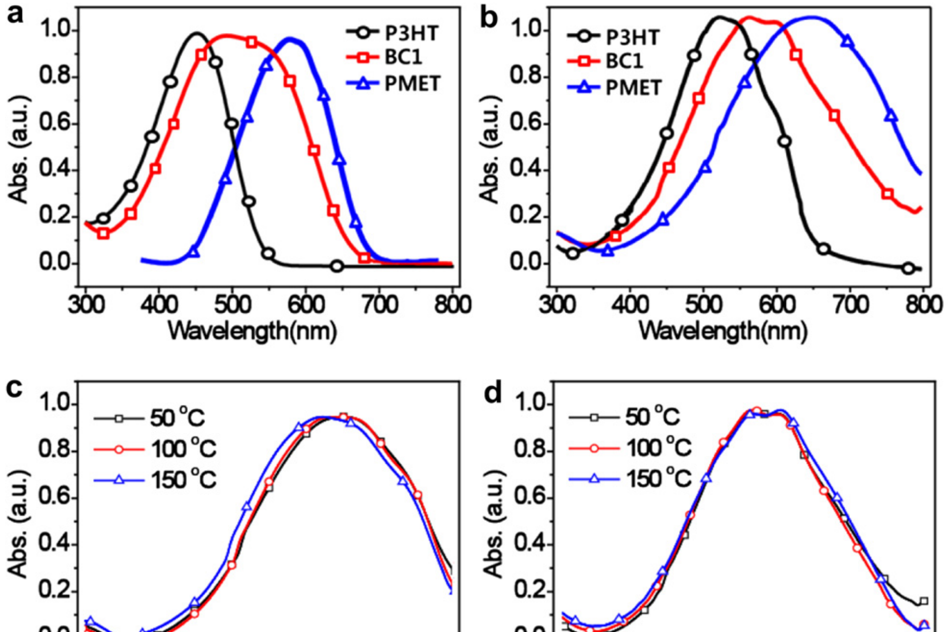

Fig. 4. Normalized UV–Vis absorption spectra. (a) P3HT, **BC1**, and PMET in chloroform. (b) P3HT, **BC1**, and PMET in film. (c) Temperature dependence of PMET in film. (d) Temperature dependence of **BC1** in film.

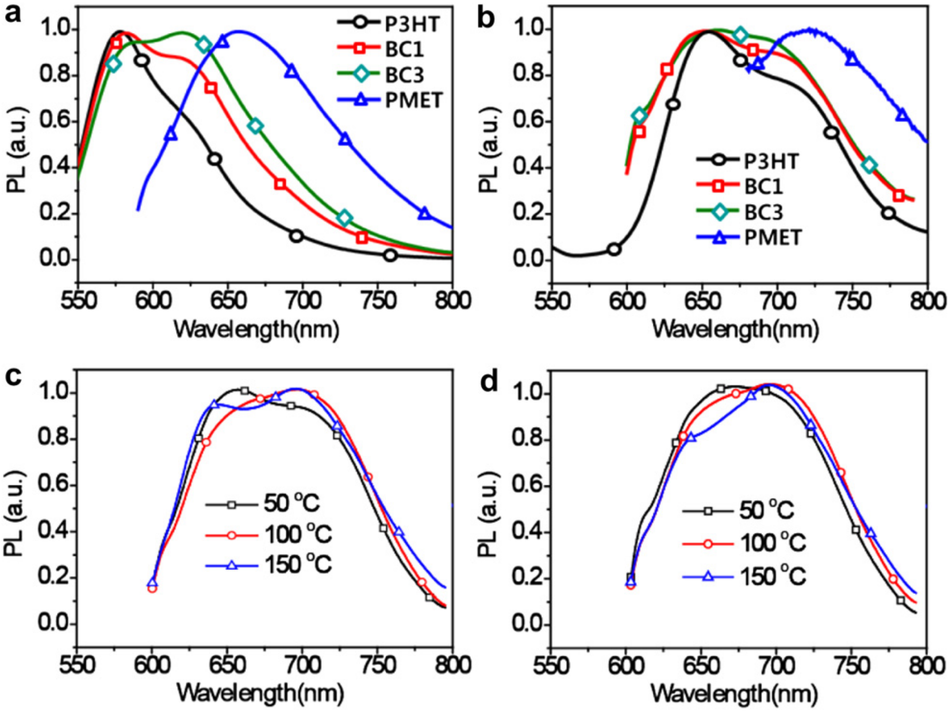

Fig. 5. Normalized photoluminescence (PL). (a) P3HT, **BC1**, **BC3**, and PMET in chloroform. (b) P3HT, **BC1**, **BC3**, and PMET in film. (c) Temperature dependence of **BC1** in films. (d) Temperature dependence of **BC3** in films.

those (578 nm in chloroform and 653 nm in film) of P3HT due to the mesomeric effect of the alkoxy side chain [17]. PMET exhibited a red shift of 64 nm at λ_{max} in transitioning from solution to film, and this red shift was 11 nm smaller than the red shift observed in P3HT. This indicated that the flexible side chains slightly hampered ordering of the PMET blocks in the copolymer, as observed by photoluminescent emission. The emission spectra of the block copolymers, **BC1** and **BC3**, showed some differences, depending on the block ratios (Fig. 5(a)). **BC1** (53% of the PMET block ratio) gave a λ_{max} of 582 nm with a shoulder at 620 nm. However, the emission at 620 nm was dominant in **BC3**, which contains 56% PMET block. This observation was ascribed to the high flexibility of the PMET block, which increased the ordering among the π-π interactions between P3HT blocks. The peak at 582 nm is characteristic of π-stacking in P3HT [19]. Similar trends were observed in the emission spectra of the film states (Fig. 5(b)). Annealing of **BC1** and **BC3** clearly demonstrated PMET block-assisted organization of the P3HT block in the copolymers, as shown in Fig. 5(c) and (d), respectively.

3.3. Electrochemical properties

The electrochemical properties of **BC1** were investigated using cyclic voltammetry (CV), and the resulting data for P3HT and PMET are summarized in Table 3. The polymer film was coated onto a glassy carbon disk by dropping the polymer solution in chloroform. The potentials were calibrated against an internal ferrocene (Fc) standard. It should be noted that the oxidation potential, measured by cyclic voltammetry, was the lowest among the independently oxidizable species in the polymer chain. Thus, the oxidation potential may be strongly affected by the electronic properties of the P3HT and PMET blocks. The PMET block of **BC1** having the alkoxy side chains on was more electron-rich than the P3HT block having the alkyl substituents. Thus, the oxidation behavior of **BC1** may be dominated by the properties of the PMET block. Indeed, the initial oxidation of **BC1** occurred at a potential (−0.22 V) at which PMET began to oxidize, even though the onset potential for **BC1** was determined to be 0.083 V, based on its major oxidation slope, as shown in Fig. 6. The oxidation potential of **BC1** at the peak maximum was 0.67 V, similar to that of P3HT (0.65 V). This result indicated that oxidation occurred separately at each block, for instance, the PMET block was oxidized at a lower voltage and the P3HT block was oxidized at a higher voltage. The block copolymers, therefore, were well-prepared. The electrochemical bandgap (ΔE_{elec}), which indicated the energy difference between

Table 3
Electrochemical properties of P3HT, PMET, and **BC1**.

	Oxidation			Reduction			
	E_{peak} (V)	E_{on} (V)	E_{HOMO} (eV)	E_{peak} (V)	E_{on} (V)	E_{LUMO} (eV)	ΔE_{elec} (eV)
P3HT	0.65	0.35	5.2	−1.45	−1.31	3.5	1.67
BC1	0.67	0.083	4.9	−1.35	−1.19	3.6	1.27
PMET	0.060	−0.22	4.6	−1.32	−1.11	3.7	0.89

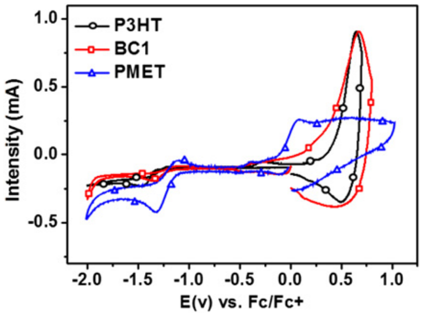

Fig. 6. Cyclic voltammograms of P3HT, PMET, and **BC1**, relative to a ferrocene internal standard.

onset potentials of oxidation and reduction, varied depending on the chemical nature of the polymer. ΔE_{elec} of PMET was 0.89 eV, which was clearly lower than that of P3HT (1.67 eV). However, discrepancies between ΔE_{elec} and ΔE_{opt} (the optical bandgap in the film) were observed, especially in **BC1**, in agreement with reports by others [20]. These discrepancies were ascribed to the hydrophilic electrolytes present during the CV measurements, although this topic requires further investigation.

4. Conclusion

We successfully synthesized thiophene-based amphiphilic all-conjugated block copolymers consisting of P3HT and PMET blocks, as confirmed by SEC measurements. The polymerization reaction via a Grignard metathesis (GRIM) in the presence of Ni(dppp)Cl_2 exhibited quasi-living characteristics, indicating the successful transfer of a catalytic site from an electron-poor precursor to an electron-rich monomer, relatively. The molecular weights of the block copolymers increased slightly with increasing polymerization temperature without decomposition of the active sites. UV–vis, PL, and CV measurements of P3HT, PMET, and the block copolymers clearly supported the association and organization of the two blocks in adjacent chains.

Acknowledgment

This work was supported by the Energy R&D program grant (20093020010040) funded by the MKE, by the Mid-career Researcher Program and the Basic Science Research Program through a National Research Foundation of Korea (NRF) grant funded by the MEST (No. 2010-0027732, No. 2009-0093462), and by the second stage of a BK21 (Brain Korea 21) grant.

Appendix. Supplementary material

Supplementary data associated with this article can be found, in the online version, at doi:10.1016/j.polymer.2011.06.030.

References

[1] McCullough RD, Williams SP, Tristram-Nagle S, Jayaraman M, Ewbank PC, Miller L. Synth Metals 1995;69:279–82.

[2] (a) Wang GM, Swensen J, Moses D, Heeger AJ. J Appl Phys 2003;93:6137–41;
(b) Sirringhaus H, Brown PJ, Friend RH, Nielsen MM, Bechgaard K, Langeveld-Voss BMW, et al. Nature 1999;401:685–8.

[3] (a) Padinger F, Rittberger RS, Sariciftci NS. Adv Funct Mater 2003;13:85–8;
(b) Ma WL, Yang CY, Gong X, Lee K, Heeger AJ. Adv Funct Mater 2005;15:1617–22;
(c) Li G, Shrotriya V, Huang JS, Yao Y, Moriarty T, Emery K, et al. Nat Mater 2005;4:864–8.

[4] (a) Thompson BC, Frëchet JM. J Angew Chem. Int Ed 2008;47:58–77;
(b) McCullough RD. Adv Mater 1998;10:93–116;
(c) Osaka I, McCullough RD. Acc Chem Res 2008;41:1202–14;
(d) Peet J, Heeger AJ, Bazan GC. Acc Chem Res 2009;42:1700–8.

[5] (a) Iovu MC, Sheina EE, Gil RR, McCullough RD. Macromolecules 2005;38:8649–56;
(b) Osaka I, McCullough RD. Acc Chem Res 2008;41:1202–14;
(c) Sheina EE, Liu J, Iovu MC, Laird DW, McCullough RD. Macromolecules 2004;37:3526–8;
(d) Loewe RS, Khersonsky SM, McCullough RD. Adv Mater 1999;11:250–3;
(e) Stefan MC, Javier AE, Osaka I, McCullough RD. Macromolecules 2009;42:30.

[6] (a) Miyakoshi R, Yokoyama A, Yokozawa T. J Am Chem Soc 2005;127:17542–7;
(b) Adachi I, Miyakoshi R, Yokoyama A, Yokozawa T. Macromolecules 2006;39:7793–5;
(c) Yokoyama A, Yokozawa T. Macromolecules 2007;40:4093–101;
(d) Yokoyama A, Miyakoshi R, Yokozawa T. Macromolecules 2004;37:1169–71;
(e) Miyakoshi R, Yokoyama T. Macromol Rapid Commun 2004;25:1663–6;
(f) Miyakoshi R, Yokoyama A, Yokozawa T. J Polym Sci. Part A Polym Chem 2008;46:753–65;
(g) Yokoyama A, Kato A, Miyakoshi R, Yokozawa T. Macromolecules 2008;41:7271–3.

[7] (a) Zhang Y, Tajima K, Hirota K, Hashimoto K. J Am Chem Soc 2008;130:7812–3;
(b) Zhang Y, Tajima K, Hashimoto K. Macromolecules 2009;42:7008–15.

[8] (a) Wu PT, Ren G, Li C, Mezzenga R, Jenekhe SA. Macromolecules 2009;42:2317–20;
(b) Ouhib F, Hiorns RC, de Bettignies R, Bailly S, Desbrières J, Dagron-Lartigau C. Thin Solid Films 2008;516:719–7104;
(c) Ohshimizu K, Ueda M. Macromolecules 2008;41:5289–9294;
(d) Wen L, Duck B, Dastoor PC, Rasmussen SC. Macromolecules 2008;41:4576–8.

[9] (a) Miyakoshi R, Yokoyama A, Yokozawa T. Chem Lett 2008;37:1022–3;
(b) Wu S, Bua L, Huang L, Yu X, Han Y, Geng Y, et al. Polymer 2009;50:6245–51.

[10] Yokoyama A, Kato A, Miyakoshi R, Yokozawa T. Macromolecules 2008;41:7271–4.

[11] Stefan MC, Javier AE, Osaka I, McCullough RD. Macromolecules 2009;42:30–2.

[12] Kim J, Song IY, Park T. Chem Commun 2011;47:4697–9.

[13] (a) Chen SA, Tsai CC. Macromolecules 1993;26:2234–9;
(b) Sheina EE, Khersonsky SM, Jones EG, McCullough RD. Chem Mater 2005;17:3317–9.

[14] Hauk D, Lang S, Murso A. Org Process Res Dev 2006;10:733–8.

[15] Lanni EL, McNeil AJ. J Am Chem Soc 2009;131:16573–9.

[16] (a) Jenekhe SA, Osaheni JA. Science 1994;265:765–8;
(b) Wang S, Wu P, Han Z. Macromolecules 2003;36:4567–76;
(c) Sannigrahi A, Arunbabu D, Sankar RM, Jana T. Macromolecules 2007;40:2844–51.

[17] Wu I-C, Lai C-H, Chen D-Y, Shih C-W, Wei C-Y, Ko B-T, et al. J Mater Chem 2008;18:4297–303.

[18] (a) Boer BD, Hutten PFV, Ouali L, Grayer V, Hadziioannou G. Macromolecules 2002;35:6883–92;
(b) Sirringhaus H, Tessler H, Friend RH. Science 1998;280:1741–4;
(c) Österbacka R, An CP, Jiang XM, Vardeny ZV. Science 2000;287:839–42.

[19] (a) Yamamoto T, Komarudin D, Arai M, Lee B, Suganuma H, Asakawa N, et al. J Am Chem Soc 1998;120:2047–58;
(b) Mena-Osteritz E, Meyer A, Langeveld-Voss BMW, Janssen RAJ, Meijer EW, Bäuerle P. Angew Chem. Int Ed 2000;39:2680–4;
(c) Kim DH, Park YD, Jang Y, Yang H, Kim YH, Han JI, et al. Adv Funct Mater 2005;15:77–82;
(d) Zhang Y, Wang C, Rothberg L, Ng MK. J Mater Chem 2006;16:3721–5.

[20] (a) Brabec CJ, Cravino A, Meissner D, Sariciftci NS, Fromherz T, Rispens MT, et al. Adv Funct Mater 2001;11:374–80;
(b) Liu B, Yu WL, Lai YH, Huang W. Chem Mater 2001;13:1984–91.